Explicit Analysis of Channel Mismatch Effects in Time-Interleaved ADC Systems

Naoki Kurosawa, Haruo Kobayashi, *Member, IEEE*, Kaoru Maruyama, Hidetake Sugawara, and Kensuke Kobayashi

Abstract—A time-interleaved A–D converter (ADC) system is an effective way to implement a high-sampling-rate ADC with relatively slow circuits. In the system, several channel ADCs operate at interleaved sampling times as if they were effectively a single ADC operating at a much higher sampling rate. However, mismatches such as offset, gain mismatches among channel ADCs as well as timing skew of the clocks distributed to them degrade *S/N* of the ADC system as a whole. This paper analyzes the channel mismatch effects in the time-interleaved ADC system. Previous analysis showed the effect for each mismatch *individually*, however in this paper we derive *explicit* formulas for the mismatch effects when *all* of offset, gain and timing mismatches exist together. We have clarified that the gain and timing mismatch effects interact with each other but the offset mismatch effect is independent from them, and this can be seen clearly in frequency domain. We also discuss the bandwidth mismatch effect. The derived formulas can be used for calibration algorithms to compensate for the channel mismatch effects.

Index Terms—A–D converter, analog circuit, calibration, channel mismatch, interleave, track/hold circuit.

I. INTRODUCTION

ELECTRONIC devices are continuously getting faster and accordingly, the need for instruments such as digitizing oscilloscopes and large scale integrated (LSI) circuit testers to measure their performance is growing. A–D converters (ADCs) incorporated in such instruments have to operate at a very high sampling rate. This paper studies theoretical issues of a time-interleaved ADC system where several channel ADCs operate at interleaved sampling times as if they were effectively a single ADC operating at a much higher sampling rate [1]–[7]. Fig. 1 shows such an ADC system where each M channel ADCs (ADC_1, ADC_2, $\ldots$, ADC_M) operates with one of M phase clocks (CK_1, CK_2, $\ldots$, CK_M), respectively. The sampling rate of the ADC as a whole is M times the channel sampling rate. This time-interleaved ADC system is an effective way to implement a high-sampling-rate ADC with relatively slow circuits, and is widely used. Ideally, characteristics of channel ADCs should be identical and clock skew should be zero. However, in reality there are mismatches such as offset, gain mismatches among channel ADCs as well as timing skew of the clocks distributed to them, which cause so-called *pattern noise* and significantly degrade *S/N* (effective bits) of the
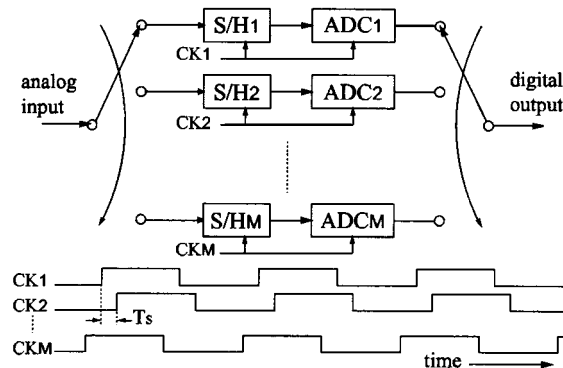
Fig. 1. Time-interleaved ADC system.

ADC system as a whole. Hence calibration often has to be incorporated to ensure uniformity among the characteristics of the channels. It is important to clarify the issues of the interleaved ADC architecture for designing the system. This channel mismatch in the interleaved ADC system may be called as *system level mismatch* or *module level mismatch*, while, for example, a random offset voltage in a CMOS differential pair circuit due to device size and threshold voltage mismatches may be called as *circuit level mismatch*.

This paper first reviews interleaving issues, the effects of offset, gain and timing mismatches *individually* [4]–[11]. Then, we will derive *explicit* formulas for the mismatch effects when all of offset, gain and timing mismatches exist together, and show that the gain and timing mismatch effects interact each other but the offset mismatch effect is independent from them. We also analyze the bandwidth mismatch effect. The derived formulas can be used for calibration algorithms to compensate for the channel mismatch effects. In this paper, we concentrate on two-channel and four-channel interleaved systems because they cover most of the practical applications. Eight-channel or others may be sometimes used in practical situation, and the extension of the results here to an interleaved system of other channels is also possible.

Hereafter, we will use following notations:

M	number of channel ADCs in the ADC system;
f_{noise}	pattern noise frequency of the ADC output;
f_{in}	input frequency applied to the ADC system;
f_s	sampling frequency of the ADC system;
f_s/M	sampling frequency of each channel ADC.

II. INDIVIDUAL CHANNEL MISMATCH EFFECTS

This section reviews the effects of offset, gain and timing mismatches *individually* in interleaved ADC systems [4]–[11].
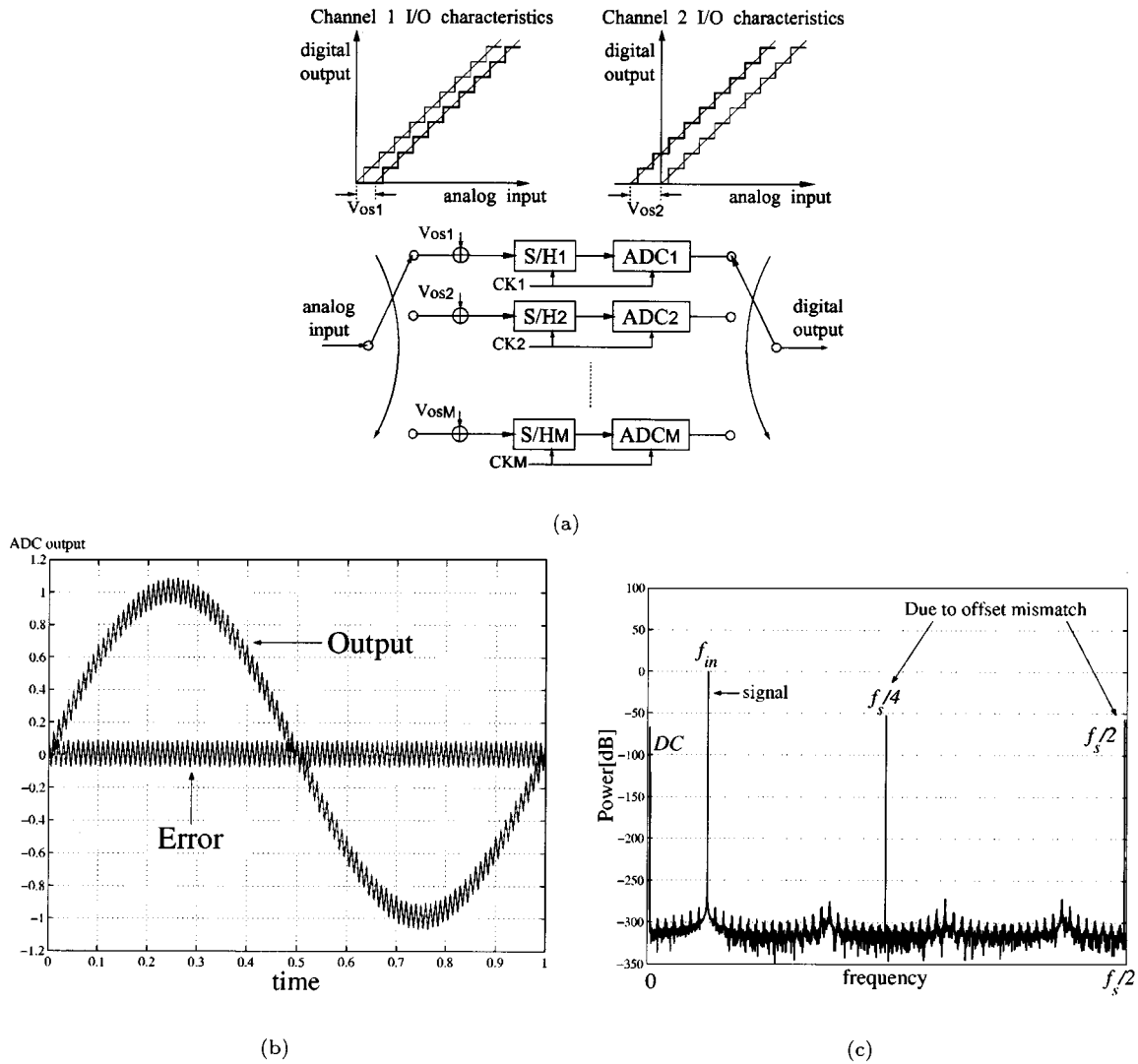
Fig. 2   Offset mismatch effect. (a) Offset mismatch model. Vos_k represents the offset of kth channel $(k = 1, 2, \cdots, M)$. (b) ADC output and error signals in time domain for a sinusoidal input. (c) ADC output power spectrum.

A. Offset Mismatch Effects

Suppose that the offsets of each channel are different and the other characteristics are identical (Fig. 2). This mismatch causes *fixed pattern noise* in the ADC system. For a dc input, each channel may produce a different output code and the period of this error signal is M/f_s. The pattern noise is almost independent of the input signal in time and frequency domains, and it is additive noise in time domain while in frequency domain it causes noise peaks at

$$f_{\text{noise}} = k \times f_s/M, \qquad k = 1, 2, 3, \ldots.$$

The *S/N* degradation of the ADC system (total pattern-noise power) due to the offset mismatch is constant regardless of the input frequency and amplitude (Fig. 3).

B. Gain Mismatch Effects

Suppose that the gains of each channel are different and the other characteristics are identical (Fig. 4). If a sinusoidal input
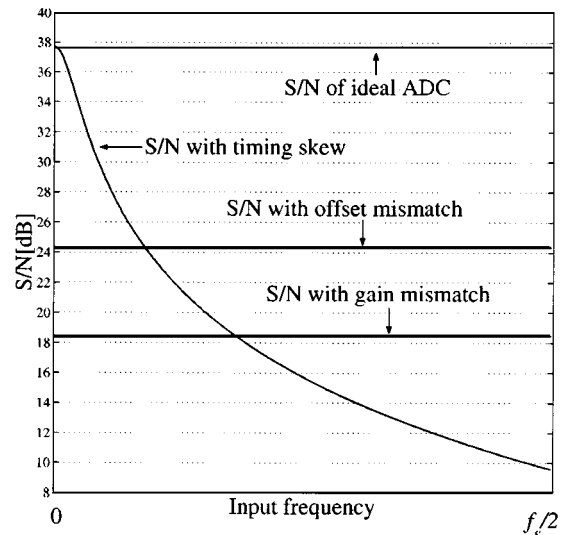

Fig. 3.   Simulation results of *S/N* versus f_{in} of a four-channel 6-bit interleaved ADC system in offset, gain and timing mismatch cases.
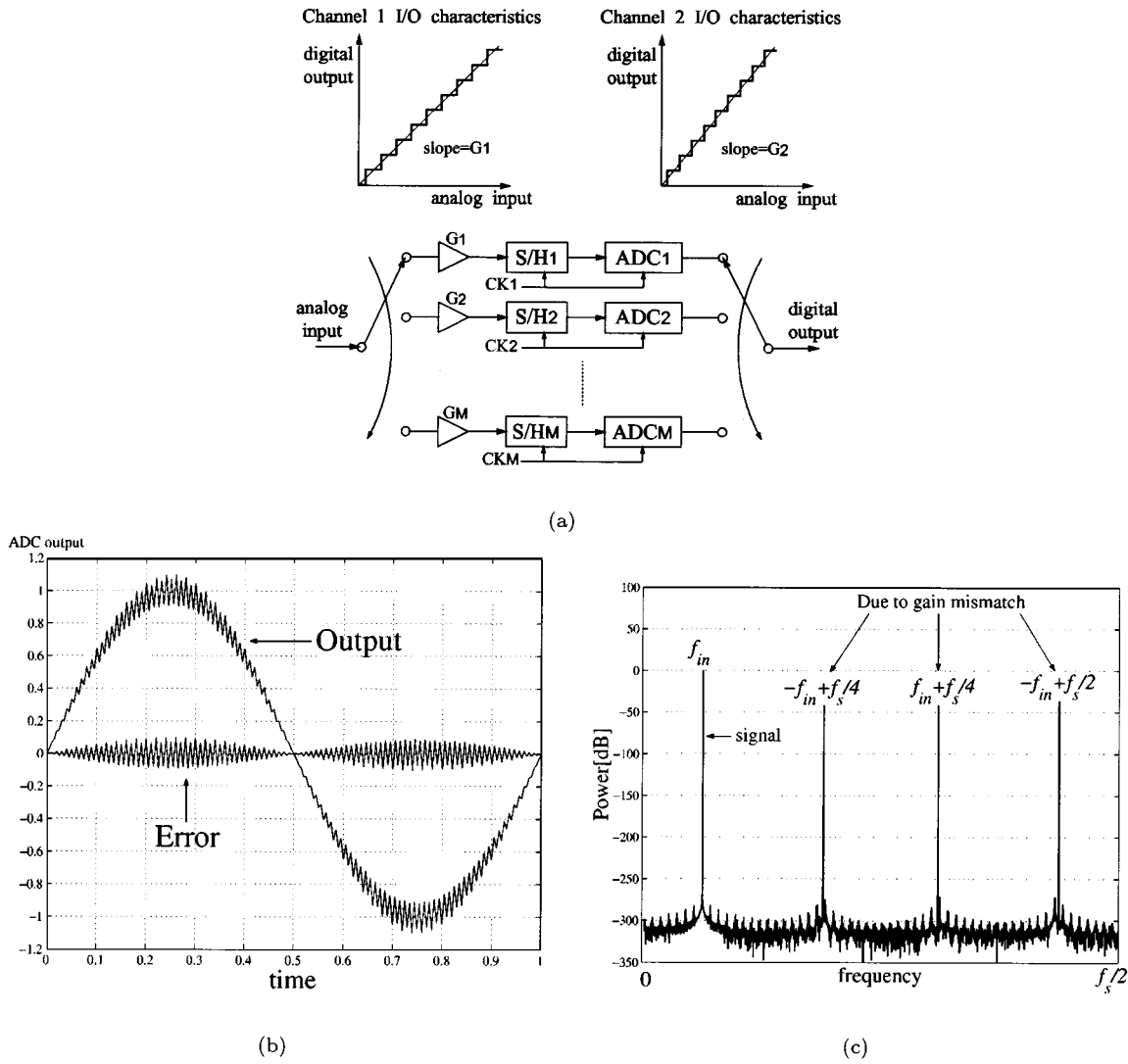
Fig. 4. Gain mismatch effect. (a) Gain mismatch model. G_k represents the gain of kth channel ($k = 1, 2, \ldots, M$). (b) ADC output and error signals in time domain for a sinusoidal input. (c) ADC output power spectrum.

signal is applied to the system, the largest difference in channel outputs occurs at the peaks of the sine wave. As with the offset mismatch case, the basic error occurs with a period of M/f_s but the magnitude of the error is modulated by the input frequency f_{in}. Thus, the pattern noise due to gain mismatch is multiplicative in time domain—which is like amplitude modulation (AM) noise—while noise spectrum peaks are at

$$f_{\text{noise}} = \pm f_{\text{in}} + \frac{k}{M} f_s, \qquad k = 1, 2, 3, \ldots.$$

f_{noise} depends on f_{in} (Fig. 4) while the *S/N* degradation of the ADC system due to the gain mismatch is independent of f_{in} (Fig. 3). Also, note that in the offset mismatch case, the *S/N* degradation (noise power) is independent of the amplitude of the input but in the gain mismatch case, it depends on the amplitude.

C. Clock Timing Error Effects

There are two kinds of timing errors in an interleaved ADC system, clock skew (systematic error) and clock jitter (random error). Clock jitter effects are unavoidable in any ADC system

but the interleaved architecture also suffers from clock skew effects. Suppose that the clocks $CK_1, CK_2, \cdots, CK_M$ have skews $dt_1, dt_2, \cdots, dt_M$ (Fig. 5). This skew causes noise in the ADC system, and in the time domain the largest error occurs when the input signal has the largest slew rate, or crosses zero, which is like phase modulation (PM) noise (Fig. 6). The envelope of the error signal is the largest at the zero-crossings with a period of M/f_s. It is shifted by 90 deg compared to the gain mismatch case. In the frequency domain, as with the gain mismatch case, the basic error occurs with a period of M/f_s and the magnitude of the error is modulated by the input frequency f_{in}. The noise spectrum peaks are at

$$f_{\text{noise}} = \pm f_{\text{in}} + \frac{k}{M} f_s, \qquad k = 1, 2, 3, \ldots.$$

Note, that *S/N* degrades as f_{in} increases (Fig. 3).

Remark: In offset and gain mismatch cases, the signal power at the output keeps constant as f_{in} increases. On the other hand, in the timing skew case, the signal power at the output decreases as f_{in} increases, while the total power of the signal and the error at the output keeps constant.
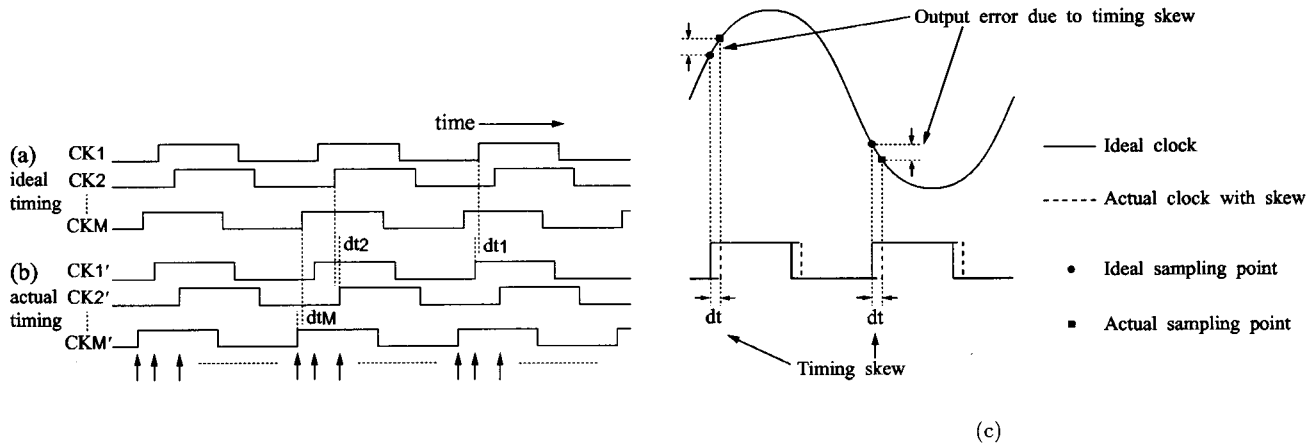
Fig. 5. Clock skew: (a) Ideal clock timing. (b) Clock timing with skews of dt_1, dt_2, ..., dt_M. (c) Timing skew causes error for the sampled data.
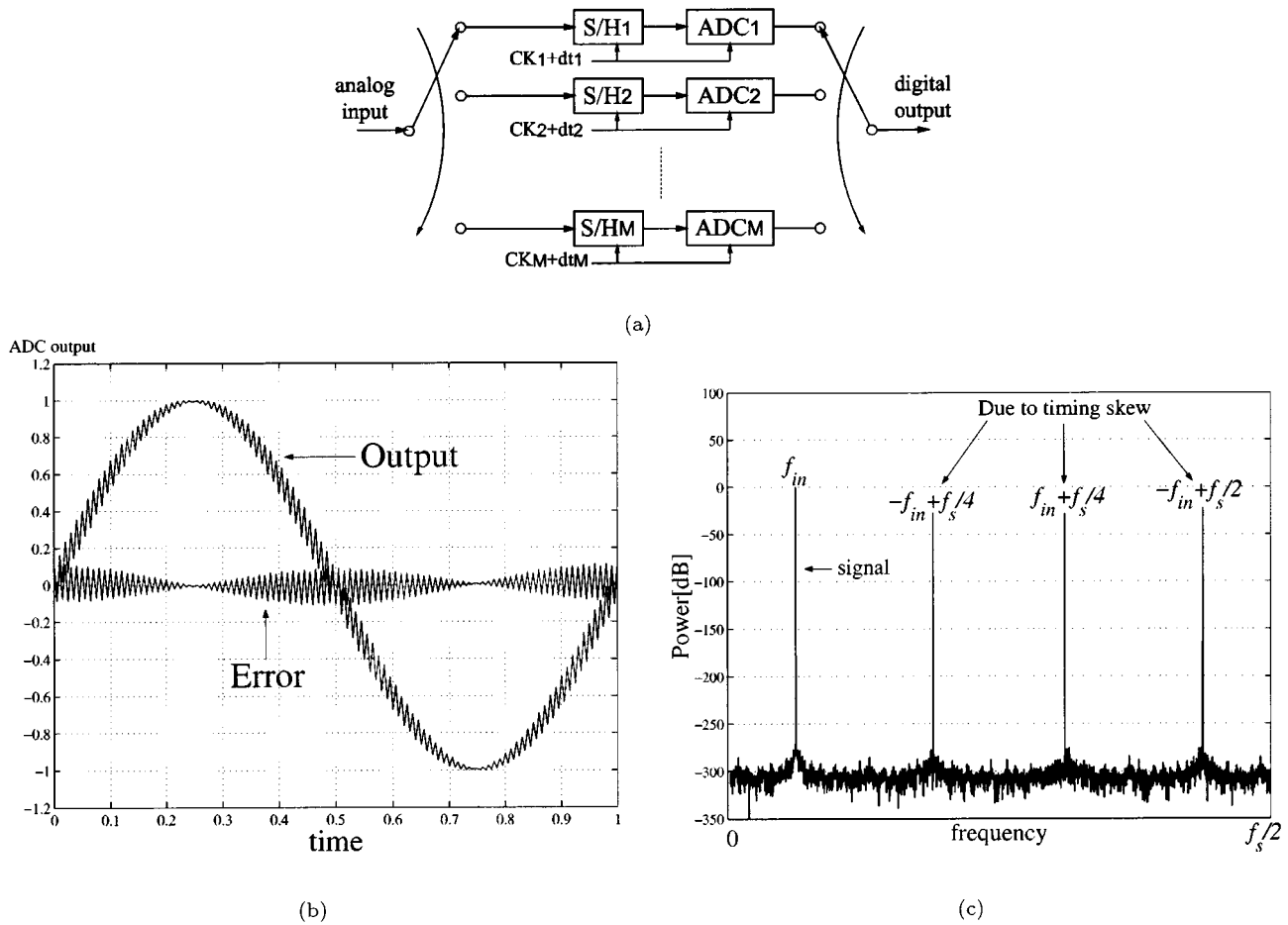

Fig. 6. Timing skew effect. (a) Timing skew model. dt_k represents the skew of kth clock $(k = 1, 2, ..., M)$. (b) ADC output and error signals in time domain for a sinusoidal input. (c) ADC output power spectrum.

III. COMBINED CHANNEL MISMATCH EFFECTS

In this section, we will derive *explicit* formulas for the mismatch effects when all of offset, gain and timing mismatches exist together, and show that the gain and timing mismatch effects interact each other but the offset mismatch effect is independent of them.

A. Two-channel Interleaved ADC $(M = 2)$

First, we consider a two-channel interleaved ADC system. Fig. 7 shows its configuration where each of two-channel ADCs (ADC$_1$, ADC$_2$) operates with one of two-phase clocks (Φ_1, Φ_2 with a period of $2T_s$), respectively. The sampling rate (f_s, where $f_s \triangleq 1/T_s$) of the ADC as a whole is twice the channel sampling rate. However, as mentioned before, this interleaved ADC
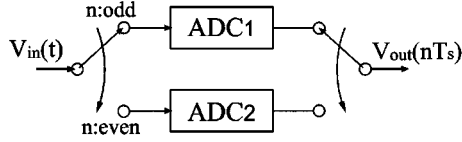
Fig. 7.   Two-channel time-interleaved ADC system.

system suffers from channel mismatch effects [8], [9], [11]: gain mismatch, offset mismatch and timing mismatch. Ideally, ADC_1 and ADC_2 should be identical. However, in reality, their gains and offsets may be different from each other, and also the sampling timings may deviate from Φ_1 and Φ_2. Let the gains of ADC_1, ADC_2 be G_1, G_2 respectively, and their offsets be os_1, os_2 respectively. Also, let the sampling timing deviations from Φ_1 for ADC_1 and Φ_2 for ADC_2 be δt_1, δt_2 respectively. Suppose that the input to the ADC is a sinusoidal signal $V_{in}(t) = A\cos(2\pi f_{in}t)$. Then, the output of the two-channel interleaved system is given as follows:

$$V_{out}(n) = \begin{cases} G_1 A\cos[2\pi f_{in}(nT_s + \delta t_1)] + os_1 & (n: \text{odd}) \\ G_2 A\cos[2\pi f_{in}(nT_s + \delta t_2)] + os_2 & (n: \text{even}). \end{cases}$$
$$(1)$$

Let

$$G \triangleq (G_1 + G_2)/2 \qquad \alpha \triangleq (G_2 - G_1)/(2G)$$
$$\delta t_{cm} \triangleq (\delta t_1 + \delta t_2)/2 \qquad \delta t \triangleq \delta t_2 - \delta t_1$$
$$os_{cm} \triangleq (os_1 + os_2)/2 \qquad os_{diff} \triangleq (os_2 - os_1)/2. \quad (2)$$

Without loss of generality, we choose the timing reference so that $\delta t_{cm} = 0$. Then, we obtain the following:

$$\begin{aligned} V_{out}(nT_s) = {} & A_s \cos(2\pi f_{in}nT_s + \theta_s) \\ & + A_n \cos\left[2\pi\left(-f_{in} + \tfrac{1}{2}f_s\right)nT_s + \theta_n\right] \\ & + os_{cm} + \cos(\pi n)os_{diff} \end{aligned} \quad (3)$$

where

$$A_s \triangleq AG\sqrt{\cos^2(\pi f_{in}\delta t) + \alpha^2 \sin^2(\pi f_{in}\delta t)}$$
$$A_n \triangleq AG\sqrt{\alpha^2 \cos^2(\pi f_{in}\delta t) + \sin^2(\pi f_{in}\delta t)}$$
$$\theta_s \triangleq \arctan[\alpha \tan(\pi f_{in}\delta t)]$$
$$\theta_n \triangleq -\arctan[\tan(\pi f_{in}\delta t)/\alpha].$$

Remark:

1) $V_{out}(nT_s)$ given by (3) has four frequency components; the frequency of the first term in (3) is f_{in}, that of the second term is $-f_{in} + (1/2)f_s$, the third one is 0 (dc) and the fourth one is $(1/2)f_s$. In other words, the first term corresponds to signal while the second term is due to gain and timing mismatches and the third term is caused by the average offset of ADC_1 and ADC_2 while the fourth term is caused by offset mismatch.

2) Equation (3) that we have newly derived considers the gain, offset and timing mismatches together and hence
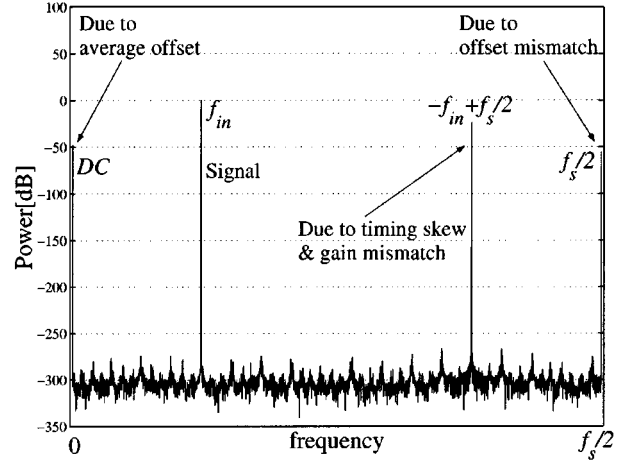

Fig. 8.   Simulation result of a two-channel time-interleaved ADC system with channel mismatches which verifies the correctness of our derived equation (3). 8192-point FFT was performed with $A = 1$, $G = 1$, $f_{in}/f_s = 997/8192$, gain mismatch of $\alpha = 0.03$, timing mismatch of $\delta t = 2.0 \times 10^{-5}$, average offset of $os_{cm} = 2.0 \times 10^{-3}$, and offset mismatch of $os_{diff} = 9.0 \times 10^{-4}$ in (1) and (2).
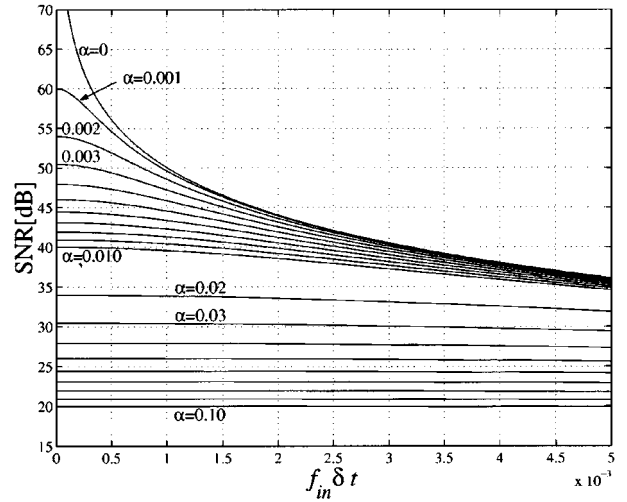

Fig. 9.   Simulation result of SNR of a two-channel interleaved ADC system with gain mismatch (α) and timing skew (δt) based on (3).

this is a very general result. However, in previous references [5], [6], [8]–[11] each channel mismatch effect in interleaved ADC systems is discussed only individually.

3) From (3) we see that the effects of gain and timing mismatch interact each other while the offset mismatch effect is independent.

4) Numerical simulations show that (1) and (3) match exactly; in both cases, the power at dc is -47.959 dB, the power and phase at f_{in} are $-0.017\,038$ dB, $0.107\,82$ deg, those at $f_{in} + f_s/2$ are -23.1736 dB, -64.439 deg and those at $f_s/2$ are -54.8945 dB, 0.0 deg with the simulation conditions in the caption of Fig. 8, where the simulated power spectrum is shown.

5) Fig. 9 shows numerical simulation result for the SNR due to gain mismatch and timing skew which would be useful for designing a two-channel interleaved system. In Fig. 9, the horizontal axis indicates timing skew δt normalized by the input frequency f_{in}, and the vertical axis shows the
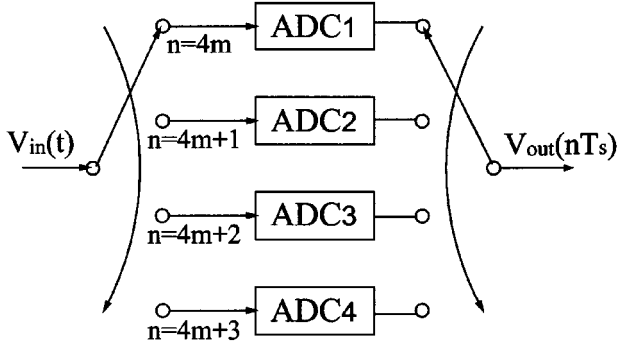
Fig. 10. Four-channel time-interleaved ADC system.

SNR of the two-channel interleaved ADC system with a parameter of gain mismatch α. For example we can see in Fig. 9 that gain matching better than 0.1% is required to obtain SNR better than 54 dB for $f_{in}\delta t \leq 0.5 \times 10^{-3}$. Note that the offset mismatch effect is not included in Fig. 9, however, it is independent of gain and timing mismatch effects and it can be simply added to them.

Fact 1: The total power P_{out1} of the signal and noise at the whole system output is given by

$$P_{out1} = \tfrac{1}{4} A^2(G_1^2 + G_2^2) + \tfrac{1}{2}(os_1^2 + os_2^2).$$

Proof: See Appendix III.

B. Four-channel Interleaved ADC $(M = 4)$

Next, we consider a four-channel interleaved ADC system, and Fig. 10 shows its configuration. Similarly, let the gains of ADC_1, ADC_2, ADC_3, ADC_4 be G_1, G_2, G_3, G_4, respectively, and their offsets be os_1, os_2, os_3, os_4, respectively. Also, let the sampling timing deviations be δt_1, δt_2 δt_3, δt_4, respectively. Suppose that the input to the ADC is a sinusoidal signal $V_{in}(t) = A\cos(2\pi f_{in}t)$. Then, the output of the four-channel interleaved system is given as follows:

$$V_{out}(n)$$
$$= \begin{cases} G_1 A\cos[2\pi f_{in}(nT_s + \delta t_1)] + os_1 & (n = 4m) \\ G_2 A\cos[2\pi f_{in}(nT_s + \delta t_2)] + os_2 & (n = 4m+1) \\ G_3 A\cos[2\pi f_{in}(nT_s + \delta t_3)] + os_3 & (n = 4m+2) \\ G_4 A\cos[2\pi f_{in}(nT_s + \delta t_4)] + os_4 & (n = 4m+3) \end{cases} \quad (4)$$

where $m = 0, \pm 1, \pm 2, \pm 3, \ldots$, and let

$$G_1 \triangleq G(1+\alpha_1) \qquad G_2 \triangleq G(1+\alpha_2)$$
$$G_3 \triangleq G(1+\alpha_3) \qquad G_4 \triangleq G(1+\alpha_4) \qquad (5)$$

where

$$G \triangleq \frac{G_1 + G_2 + G_3 + G_4}{4}.$$

Without loss of generality, we choose the timing reference so that

$$\delta t_1 + \delta t_2 + \delta t_3 + \delta t_4 = 0.$$

Then, we obtain the following:

$$V_{out}(nT_s)$$
$$= A_{s4}\cos\left(2\pi f_{in}nT_s - \arctan\frac{A_{ss}}{A_{sc}}\right)$$
$$+ A_{n1}\cos\left[2\pi nT_s\left(f_{in} + \frac{1}{4}f_s\right) - \arctan\frac{A_{n1s}}{A_{n1c}}\right]$$
$$+ A_{n2}\cos\left[2\pi nT_s\left(f_{in} + \frac{1}{2}f_s\right) - \arctan\frac{A_{n2s}}{A_{n2c}}\right]$$
$$+ A_{n3}\cos\left[2\pi nT_s\left(f_{in} + \frac{3}{4}f_s\right) - \arctan\frac{A_{n3s}}{A_{n3c}}\right]$$
$$+ \tfrac{1}{4}(os_1 - os_2 + os_3 - os_4)\cos\left[2\pi nT_s\left(\tfrac{1}{2}f_s\right)\right]$$
$$+ \tfrac{1}{2}\sqrt{(os_1 - os_3)^2 + (os_2 - os_4)^2}$$
$$\times \cos\left[2\pi nT_s\left(\tfrac{1}{4}f_s\right) - \arctan\frac{os_2 - os_4}{os_1 - os_3}\right]$$
$$+ (os_1 + os_2 + os_3 + os_4)/4 \qquad (6)$$

where

$$A_{s4} \triangleq \sqrt{A_{sc}^2 + A_{ss}^2} \qquad A_{n1} \triangleq \sqrt{A_{n1c}^2 + A_{n1s}^2}$$
$$A_{n2} \triangleq \sqrt{A_{n2c}^2 + A_{n2s}^2} \qquad A_{n3} \triangleq \sqrt{A_{n3c}^2 + A_{n3s}^2}$$

and $A_{sc}, A_{ss}, A_{n1c}, A_{n1s}, A_{n2c}, A_{n2s}, A_{n3c}, A_{n3s}$ are defined in Appendix I.

Remark:

1) Similar arguments described in two-channel case are valid for the four-channel case.
2) Numerical simulation shows that (4) and (6) match exactly; in both cases, the power at dc is -66.021[dB], the power and phase at f_{in} are $-0.041\,198$ [dB], $0.092\,319\,9$ [deg], those at $-f_{in} + f_s/4$ are -27.164 [dB], 73.792 [deg], those at $f_s/4$ are -52.041 [dB], 0.0 [deg], those at $-f_{in} + f_s/2$ are -21.945 [dB], 80.336 [deg], those at $f_{in} + 3f_s/4$ are -28.296 [dB], -84.706 [deg] and those at $f_s/2$ are -56.478 [dB], 0.0 [deg] with the simulation conditions in the caption of Fig. 11, where the simulated power spectrum is shown.
3) Fig. 12 shows numerical simulation result for the SNR due to the gain mismatch and timing skew which would be useful for designing a four-channel interleaved system, as similar to Fig. 9 in two-channel case.

Fact 2: The total power P_{out2} of the signal and noise at the whole system output is given by

$$P_{out2} = \tfrac{1}{8} A^2(G_1^2 + G_2^2 + G_3^2 + G_4^2)$$
$$+ \tfrac{1}{4}(os_1^2 + os_2^2 + os_3^2 + os_4^2).$$

Proof: See Appendix III

IV. BANDWIDTH MISMATCH EFFECT

In this section, we will introduce a rather new problem, *bandwidth mismatch*, in an interleaved ADC or an interleaved sampling system, and then we will derive the explicit formulas for its effects. Many electrical circuits can be approximated by a
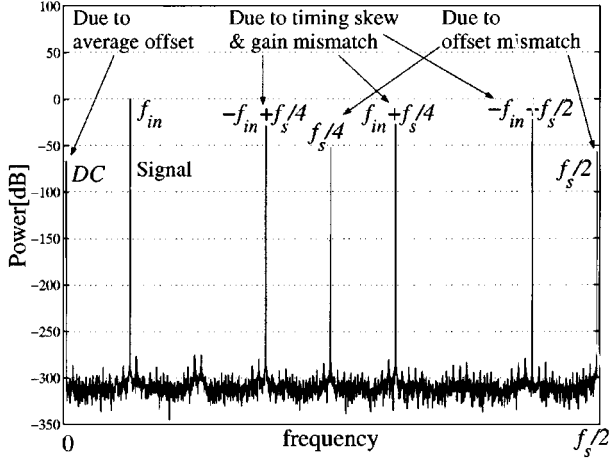
Fig. 11. Simulation result of a four-channel time-interleaved ADC system with channel mismatches which verifies the correctness of our derived equation (6). 8192-point FFT was performed with $A = 1$, $G = 1$, $f_{\rm in}/f_s = 499/8192$, gain mismatches of ($\alpha_1 = 0.03$, $\alpha_2 = -0.02$, $\alpha_3 = 0.0$ and $\alpha_4 = -0.01$), timing mismatches of ($\delta t_1 = 5.0 \times 10^{-5}$, $\delta t_2 = -2.0 \times 10^{-5}$, $\delta t_3 = 0.0$ and $\delta t_4 = -3.0 \times 10^{-5}$), and offset mismatches of ($os_1 = 2.0 \times 10^{-3}$, $os_2 = 1.0 \times 10^{-3}$, $os_4 = -3.0 \times 10^{-3}$ and $os_5 = 1.0 \times 10^{-3}$) in eqs. (4) and (5).
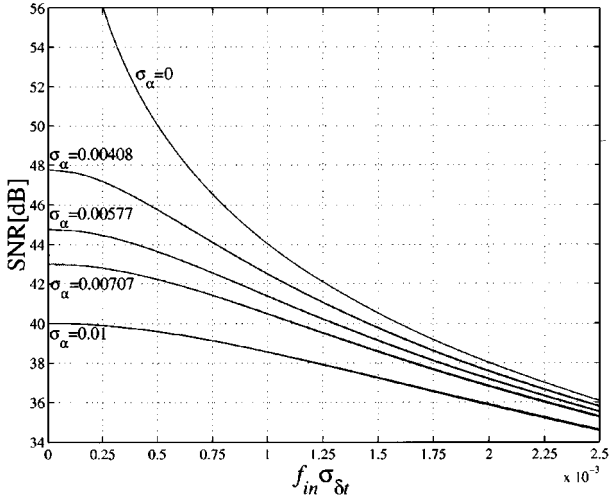

Fig. 12. Simulation result of SNR of a four-channel interleaved ADC system with gain mismatch (gain deviation of $\sigma_\alpha \triangleq \sqrt{(\alpha_1^2 + \alpha_2^2 + \alpha_3^2 + \alpha_4^2)/4}$) and timing skew (timing skew deviation of $\sigma_{\delta t} \triangleq \sqrt{(\delta t_1^2 + \delta t_2^2 + \delta t_3^2 + \delta t_4^2)/4}$) based on equation (6).

first-order system (Fig. 13). A typical example is an open-loop track/hold circuit in track mode, where the ON-resistance of the sampling switch and the hold capacitor constitute a first-order RC circuit. Here we assume that kth channel ADC is approximated by a first-order system and its bandwidth is given by f_{ck}, which can be mismatched among channels while there are no mismatches of offset, dc gain and timing discussed in the previous sections. (The reader may argue that the approximation of an ADC to a first-order system might be too inaccurate, however, for a track/hold circuit in track mode this approximation is very reasonable and hence the discussion in this section is applicable at least to interleaved sampling systems which consist of an array of track/hold circuits.) Setting the dc gain of
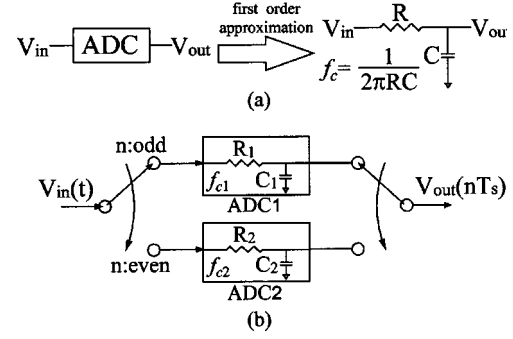

Fig. 13. Bandwidth mismatch model. (a) Approximation of an ADC to the first-order system. (b) Bandwidth mismatch model in two-channel case.

each channel to one, without loss of generality, and then the frequency transfer function $H_k(j2\pi f)$ of kth channel is given by

$$H_k(j2\pi f) = 1/(1 + jf/f_{ck})$$

and for the input of $V_{\rm in}(t) = A\cos(2\pi f_{\rm in}t)$, the output $V_{{\rm out}k}(nT_s)$ of kth channel is given by

$$V_{{\rm out}k}(nT_s) = G_k A\cos(2\pi f_{\rm in}nT_s + \theta_k)$$

where

$$G_k = 1 \left/ \sqrt{1 + (f_{\rm in}/f_{ck})^2}\right. \tag{7}$$

$$\theta_k = -\arctan(f_{\rm in}/f_{ck}). \tag{8}$$

We see that the mismatch of the bandwidth f_{ck} among channels ($k = 1, 2, \cdots, n$) causes G_k and θ_k mismatches. Note that G_k and θ_k are functions of the input frequency $f_{\rm in}$ as well as the bandwidth f_{ck}, and also note that when $f_{\rm in} = 0$, $G_k = 1$ and $\theta_k = 0$. Then, we will call the mismatch of G_k as *ac gain mismatch* and also the mismatch of θ_k as *ac phase mismatch*. Remark that the ac gain mismatch is different from the gain mismatch discussed in Sections II and III in that ac gain mismatch depends on $f_{\rm in}$ but the gain mismatch discussed before does not. Also, note that the ac phase mismatch due to the bandwidth mismatch is a *nonlinear* function of the input frequency $f_{\rm in}$ while the phase mismatch due to the timing skew is its *linear* function.

A. Two-Channel Interleaved ADC ($M = 2$)

We consider a two-channel interleaved ADC system, where the bandwidth of each channel is given by f_{c1} and f_{c2} respectively [Fig. 13(b)]. Then, when an input of $V_{\rm in}(t) = A\cos(2\pi f_{\rm in}t)$ is applied, the output of the interleaved system is given by

$$V_{\rm out}(n) = \begin{cases} G_1 A\cos(2\pi f_{\rm in}nT_s + \theta_1) & (n: {\rm odd}) \\ G_2 A\cos(2\pi f_{\rm in}nT_s + \theta_2) & (n: {\rm even}) \end{cases} \tag{9}$$

where G_1, G_2, θ_1 and θ_2 are defined in (7) and (8). Then we can obtain the following formulas:

$$V_{\rm out}(nT_s) = B_s\cos(2\pi f_{\rm in}nT_s + \theta_s)$$
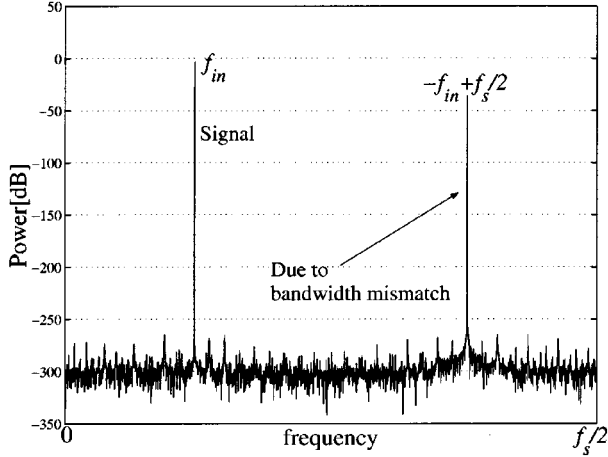$$+ B_n\cos[2\pi(-f_{\rm in} + f_s/2)nT_s + \theta_n] \tag{10}$$

Fig. 14. Simulation result of a two-channel time-interleaved ADC system with bandwidth mismatch which verifies the correctness of our derived equation (10). Here $A = 1$, $f_{c1}/f_s = 3200/(8192\pi)$, $f_{c2}/f_s = 3000/(8192\pi)$, $f_{in}/f_s = 997/8192$ are used, and 8192-point FFT is performed.
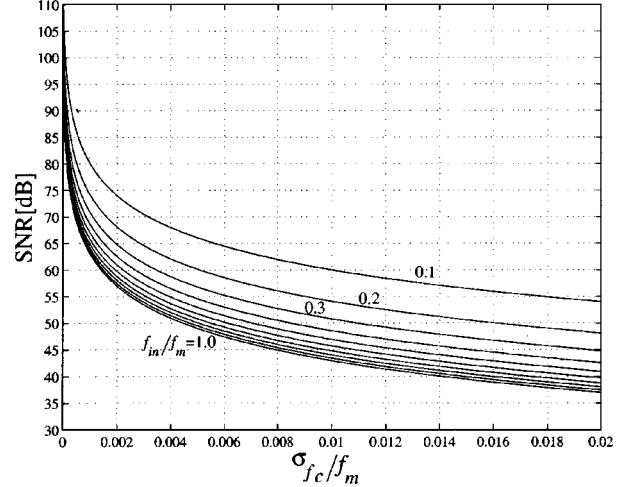

Fig. 15. Simulation result of SNR of a two-channel interleaved ADC system with bandwidth mismatch based on (10). Here, $f_m \triangleq (f_{c1} + f_{c2})/2$ (average cut-off frequency) and $\sigma_{fc} \triangleq |f_{c1} - f_{c2}|/2$ (cut-off frequency deviation between two channels). $f_{in}/f_s = 997/8192$ is used and 8192-point FFT is performed.

where

$$B_s \triangleq \frac{1}{2} A \sqrt{G_c^2 \cos^2(\theta_d) + G_d^2 \sin^2(\theta_d)}$$

$$B_n \triangleq \frac{1}{2} A \sqrt{G_c^2 \sin^2(\theta_d) + G_d^2 \cos^2(\theta_d)}$$

$$\theta_s \triangleq \arctan\left[\frac{G_c \sin(\theta_c)\cos(\theta_d) + G_d \cos(\theta_c)\sin(\theta_d)}{G_c \cos(\theta_c)\cos(\theta_d) - G_d \sin(\theta_c)\sin(\theta_d)}\right]$$

$$\theta_n \triangleq \arctan\left[\frac{G_c \cos(\theta_c)\sin(\theta_d) + G_d \sin(\theta_c)\cos(\theta_d)}{G_c \sin(\theta_c)\sin(\theta_d) - G_d \cos(\theta_c)\cos(\theta_d)}\right]$$

$$G_d \triangleq G_1 - G_2 \qquad G_c \triangleq G_1 + G_2$$

$$\theta_d \triangleq (\theta_1 - \theta_2)/2 \qquad \theta_c \triangleq (\theta_1 + \theta_2)/2.$$

Also, SNR due to the bandwith mismatch is given by

$$\text{SNR} = 10 \log_{10}(B_s^2/B_n^2) \text{ dB}.$$

Remark:

1) Numerical simulation shows that (9) and (10) match exactly; in both cases the power and phase at f_{in} are -2.8844 [dB], -44.127 [deg] and that at $-f_{in} + f_s/2$ is -35.852 [dB], -1.7165 [deg]. with the simulation conditions in the caption of Fig. 14, where the simulated power spectrum is shown.
2) Fig. 15 shows numerical simulation result for SNR versus $|f_{c1} - f_{c2}|/(f_{c1} + f_{c2})$ due to the bandwidth mismatch, which would be useful for the designer to know how much bandwidth mismatch is tolerable for a specified SNR. Note that our simulation shows that SNR does not depend on f_{in}/f_s.

Fact 3: The total power P_{out3} of the signal and noise at the whole system output is given by

$$P_{out3} = \frac{1}{4} A^2 \left[\frac{1}{1 + (f_{in}/f_{c1})^2} + \frac{1}{1 + (f_{in}/f_{c2})^2}\right].$$

Proof: See Appendix III.

B. Four-channel Interleaved ADC $(M = 4)$

Next, we consider a four-channel interleaved ADC system, where the bandwidth of each channel is given by f_{c1}, f_{c2} f_{c3} and f_{c4} respectively. Then when the input of $V_{in}(t) = A\cos(2\pi f_{in}t + \theta)$ is applied, the output of the interleaved system is given by

$$V_{out}(nT_s) = \begin{cases} G_1 A \cos(2\pi f_{in}nT_s + \theta_1) & (n = 4m) \\ G_2 A \cos(2\pi f_{in}nT_s + \theta_2) & (n = 4m+1) \\ G_3 A \cos(2\pi f_{in}nT_s + \theta_3) & (n = 4m+2) \\ G_4 A \cos(2\pi f_{in}nT_s + \theta_4) & (n = 4m+3) \end{cases}$$
(11)

where

$$\theta + \frac{1}{4}(\theta_1 + \theta_2 + \theta_3 + \theta_4) = 0$$

and $G_1, G_2, G_3, G_4, \theta_1, \theta_2, \theta_3$ and θ_4 are defined in (7) and (8). Then, we can obtain the following formulas:

$$
\begin{aligned}
V_{out}&(nT_s) \\
&= B_{s4} \cos\left[2\pi f_{in}nT_s - \arctan\frac{B_{ss}}{B_{sc}}\right] \\
&\quad + B_{n1} \cos\left[2\pi\left(f_{in} + \frac{1}{4}f_s\right)nT_s - \arctan\frac{B_{n1s}}{B_{n1c}}\right] \\
&\quad + B_{n2} \cos\left[2\pi\left(f_{in} + \frac{1}{2}f_s\right)nT_s - \arctan\frac{B_{n2s}}{B_{n2c}}\right] \\
&\quad + B_{n3} \cos\left[2\pi\left(f_{in} + \frac{3}{4}f_s\right)nT_s - \arctan\frac{B_{n3s}}{B_{n3c}}\right]
\end{aligned}
$$
(12)

where

$$B_{s4} \triangleq \sqrt{B_{sc}^2 + B_{ss}^2} \qquad B_{n1} \triangleq \sqrt{B_{n1c}^2 + B_{n1s}^2}$$

$$B_{n2} \triangleq \sqrt{B_{n2c}^2 + B_{n2s}^2} \qquad B_{n3} \triangleq \sqrt{B_{n3c}^2 + B_{n3s}^2}$$
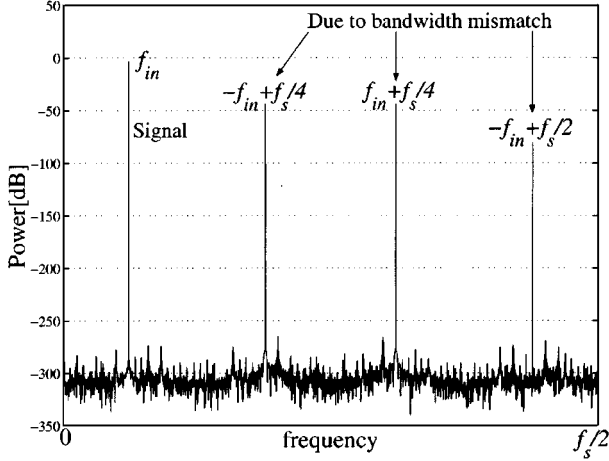
Fig. 16. Simulation result of a four-channel time-interleaved ADC system with bandwidth mismatch which verifies the correctness of our derived equation. (12). Here, $A = 1$, $f_{c1}/f_s = 1575/(8192\pi)$, $f_{c2}/f_s = 1600/(8192\pi)$, $f_{c3}/f_s = 1550/(8192\pi)$, $f_{c4}/f_s = 1525/(8192\pi)$, $f_{in}/f_s = 499/8192$ are used, and 8192-point FFT is performed.
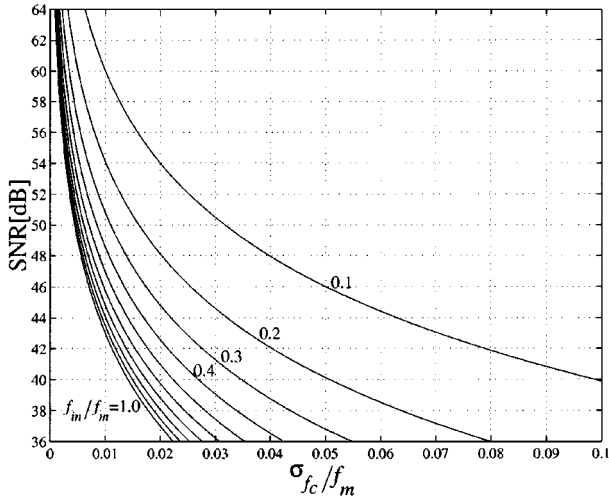

Fig. 17. Simulation result of SNR of a four-channel interleaved ADC system with bandwidth mismatch based on (12). Here we consider the case that $f_{c1} < f_{c2} < f_{c3} < f_{c4}$ and $f_{c2} - f_{c1} = f_{c3} - f_{c2} = f_{c4} - f_{c3}$. In the graph $f_m \triangleq (f_{c1} + f_{c2} + f_{c3} + f_{c4})/4$ (average cut-off frequency) and $\sigma_{f_c} \triangleq \sqrt{(f_{c1} - f_m)^2 + (f_{c2} - f_m)^2 + (f_{c3} - f_m)^2 + (f_{c4} - f_m)^2)/4}$ (cut-off frequency deviation among four channels). 8192-point FFT is performed, and $f_{in}/f_s = 997/8192$ is used.

and B_{sc}, B_{ss}, B_{n1c}, B_{n1s}, B_{n2c}, B_{n2s}, B_{n3c} and B_{n3s} are defined in Appendix II. The SNR is given by

$$\text{SNR} = 10 \log_{10} \frac{B_s^2}{B_{n1}^2 + B_{n2}^2 + B_{n3}^2} \text{ dB.}$$

Remark:

1) Numerical simulation shows that (11) and (12) match exactly; in both cases, the power and phase at f_{in} are -3.0260 [dB], $0.004\,601\,13$ [deg], those at $-f_{in} + f_s/4$ are -43.980 [dB], -26.670 [deg], those at $-f_{in} + f_s/2$ are -80.880 [dB], $-0.202\,41$[deg] and those at $-f_{in} + 3f_s/4$ are -43.979 [dB], -63.540 [deg] with the simulation conditions in the caption of Fig. 16, where the simulated power spectrum is shown.

2) Fig. 17 shows numerical simulation result for SNR versus (cut-off frequency deviation among four channels)/(average cut-off frequency) due to the bandwidth mismatch, which would be useful for the designer to know how much bandwidth mismatch is tolerable for a specified SNR. Note that our simulation shows that SNR does not depend on f_{in}/f_s.

Fact 4: The total power P_{out4} of the signal and noise at the whole system output is given by

$$P_{out4} = \frac{1}{8} A^2 \left[\frac{1}{1 + (f_{in}/f_{c1})^2} + \frac{1}{1 + (f_{in}/f_{c2})^2} + \frac{1}{1 + (f_{in}/f_{c3})^2} + \frac{1}{1 + (f_{in}/f_{c4})^2} \right].$$

Proof: See Appendix III.

V. CONCLUSION

We have analyzed the channel mismatch effects in the time-interleaved ADC system, and derived *explicit* formulas for the mismatch effects when *all* of offset, gain and timing mismatches exist together. We have clarified that the gain and timing mismatch effects interact with each other but the offset mismatch effect is independent of them. Also, we discussed the bandwidth mismatch effect (ac mismatch effect). We have shown several graphs calculated from these formulas, which are useful for the designer to know how much mismatch is tolerable for a specified SNR. Finally, we remark that we are investigating the following as on-going projects for the time-interleaved ADC system:

- Combined channel mismatch effects for all four of offset, gain, timing and bandwidth.
- Channel linearity mismatch effects.[12]
- Algorithms to measure mismatch values and compensate for them.

APPENDIX I

This appendix gives definitions of A_{sc}, A_{ss}, A_{n1c}, A_{n1s}, A_{n2c}, A_{n2s}, A_{n3c}, and A_{n3s} used in Section III-B.

$$A_{sc} \triangleq + \frac{1}{4} A(G_1 + G_3) \cos(\phi) \cos(\phi_{13})$$
$$+ \frac{1}{4} A(G_2 + G_4) \cos(\phi) \cos(\phi_{24})$$
$$- \frac{1}{4} A(G_1 - G_3) \sin(\phi) \sin(\phi_{13})$$
$$+ \frac{1}{4} A(G_2 - G_4) \sin(\phi) \sin(\phi_{24})$$

$$A_{ss} \triangleq - \frac{1}{4} A(G_1 + G_3) \sin(\phi) \cos(\phi_{13})$$
$$+ \frac{1}{4} A(G_2 + G_4) \sin(\phi) \cos(\phi_{24})$$
$$- \frac{1}{4} A(G_1 - G_3) \cos(\phi) \sin(\phi_{13})$$
$$- \frac{1}{4} A(G_2 - G_4) \cos(\phi) \sin(\phi_{24})$$

$$A_{n1c} \triangleq - \frac{1}{4} A(G_1 + G_3) \sin(\phi) \sin(\phi_{13})$$
$$+ \frac{1}{4} A(G_2 + G_4) \cos(\phi) \sin(\phi_{24})$$
$$+ \frac{1}{4} A(G_1 - G_3) \cos(\phi) \cos(\phi_{13})$$
$$- \frac{1}{4} A(G_2 - G_4) \sin(\phi) \cos(\phi_{24})$$

$$
\begin{aligned}
A_{n1s} \triangleq &-\tfrac{1}{4}A(G_1+G_3)\cos(\phi)\sin(\phi_{13})\\
&+\tfrac{1}{4}A(G_2+G_4)\sin(\phi)\sin(\phi_{24})\\
&-\tfrac{1}{4}A(G_1-G_3)\sin(\phi)\cos(\phi_{13})\\
&+\tfrac{1}{4}A(G_2-G_4)\cos(\phi)\cos(\phi_{24})
\end{aligned}
$$

$$
\begin{aligned}
A_{n2c} \triangleq &+\tfrac{1}{4}A(G_1+G_3)\cos(\phi)\cos(\phi_{13})\\
&-\tfrac{1}{4}A(G_2+G_4)\cos(\phi)\cos(\phi_{24})\\
&-\tfrac{1}{4}A(G_1-G_3)\sin(\phi)\sin(\phi_{13})\\
&-\tfrac{1}{4}A(G_2-G_4)\sin(\phi)\sin(\phi_{24})
\end{aligned}
$$

$$
\begin{aligned}
A_{n2s} \triangleq &-\tfrac{1}{4}A(G_1+G_3)\sin(\phi)\cos(\phi_{13})\\
&-\tfrac{1}{4}A(G_2+G_4)\sin(\phi)\cos(\phi_{24})\\
&-\tfrac{1}{4}A(G_1-G_3)\cos(\phi)\sin(\phi_{13})\\
&+\tfrac{1}{4}A(G_2-G_4)\cos(\phi)\sin(\phi_{24})
\end{aligned}
$$

$$
\begin{aligned}
A_{n3c} \triangleq &-\tfrac{1}{4}A(G_1+G_3)\sin(\phi)\sin(\phi_{13})\\
&-\tfrac{1}{4}A(G_2+G_4)\cos(\phi)\sin(\phi_{24})\\
&+\tfrac{1}{4}A(G_1-G_3)\cos(\phi)\cos(\phi_{13})\\
&+\tfrac{1}{4}A(G_2-G_4)\sin(\phi)\cos(\phi_{24})
\end{aligned}
$$

$$
\begin{aligned}
A_{n3s} \triangleq &-\tfrac{1}{4}A(G_1+G_3)\cos(\phi)\sin(\phi_{13})\\
&-\tfrac{1}{4}A(G_2+G_4)\sin(\phi)\sin(\phi_{24})\\
&-\tfrac{1}{4}A(G_1-G_3)\sin(\phi)\cos(\phi_{13})\\
&-\tfrac{1}{4}A(G_2-G_4)\cos(\phi)\cos(\phi_{24})
\end{aligned}
$$

where

$$
\begin{aligned}
\phi &\triangleq \tfrac{1}{2}\pi f_{\text{in}}(\delta t_1-\delta t_2+\delta t_3-\delta t_4)\\
\phi_{13} &\triangleq \pi f_{\text{in}}(\delta t_1-\delta t_3) \qquad \phi_{24} \triangleq \pi f_{\text{in}}(\delta t_2-\delta t_4).
\end{aligned}
$$

APPENDIX II

This appendix gives definitions of B_{sc}, B_{ss}, B_{n1c}, B_{n1s}, B_{n2c}, B_{n2s}, B_{n3c} and B_{n3s} used in Section IV-B.

$$
\begin{aligned}
B_{sc} \triangleq &+\tfrac{1}{4}A(G_1+G_3)\cos(\theta)\cos(\theta_{13})\\
&+\tfrac{1}{4}A(G_2+G_4)\cos(\theta)\cos(\theta_{24})\\
&-\tfrac{1}{4}A(G_1-G_3)\sin(\theta)\sin(\theta_{13})\\
&+\tfrac{1}{4}A(G_2-G_4)\sin(\theta)\sin(\theta_{24})
\end{aligned}
$$

$$
\begin{aligned}
B_{ss} \triangleq &-\tfrac{1}{4}A(G_1+G_3)\sin(\theta)\cos(\theta_{13})\\
&+\tfrac{1}{4}A(G_2+G_4)\sin(\theta)\cos(\theta_{24})\\
&-\tfrac{1}{4}A(G_1-G_3)\cos(\theta)\sin(\theta_{13})\\
&-\tfrac{1}{4}A(G_2-G_4)\cos(\theta)\sin(\theta_{24})
\end{aligned}
$$

$$
\begin{aligned}
B_{n1c} \triangleq &-\tfrac{1}{4}A(G_1+G_3)\sin(\theta)\sin(\theta_{13})\\
&+\tfrac{1}{4}A(G_2+G_4)\cos(\theta)\sin(\theta_{24})\\
&+\tfrac{1}{4}A(G_1-G_3)\cos(\theta)\cos(\theta_{13})\\
&-\tfrac{1}{4}A(G_2-G_4)\sin(\theta)\cos(\theta_{24})
\end{aligned}
$$

$$
\begin{aligned}
B_{n1s} \triangleq &-\tfrac{1}{4}A(G_1+G_3)\cos(\theta)\sin(\theta_{13})\\
&+\tfrac{1}{4}A(G_2+G_4)\sin(\theta)\sin(\theta_{24})\\
&-\tfrac{1}{4}A(G_1-G_3)\sin(\theta)\cos(\theta_{13})\\
&+\tfrac{1}{4}A(G_2-G_4)\cos(\theta)\cos(\theta_{24})
\end{aligned}
$$

$$
\begin{aligned}
B_{n2c} \triangleq &+\tfrac{1}{4}A(G_1+G_3)\cos(\theta)\cos(\theta_{13})\\
&-\tfrac{1}{4}A(G_2+G_4)\cos(\theta)\cos(\theta_{24})\\
&-\tfrac{1}{4}A(G_1-G_3)\sin(\theta)\sin(\theta_{13})\\
&-\tfrac{1}{4}A(G_2-G_4)\sin(\theta)\sin(\theta_{24})
\end{aligned}
$$

$$
\begin{aligned}
B_{n2s} \triangleq &-\tfrac{1}{4}A(G_1+G_3)\sin(\theta)\cos(\theta_{13})\\
&-\tfrac{1}{4}A_4(G_2+G_4)\sin(\theta)\cos(\theta_{24})\\
&-\tfrac{1}{4}A(G_1-G_3)\cos(\theta)\sin(\theta_{13})\\
&+\tfrac{1}{4}A(G_2-G_4)\cos(\theta)\sin(\theta_{24})
\end{aligned}
$$

$$
\begin{aligned}
B_{n3c} \triangleq &-\tfrac{1}{4}A(G_1+G_3)\sin(\theta)\sin(\theta_{13})\\
&-\tfrac{1}{4}A(G_2+G_4)\cos(\theta)\sin(\theta_{24})\\
&+\tfrac{1}{4}A(G_1-G_3)\cos(\theta)\cos(\theta_{13})\\
&+\tfrac{1}{4}A(G_2-G_4)\sin(\theta)\cos(\theta_{24})
\end{aligned}
$$

$$
\begin{aligned}
B_{n3s} \triangleq &-\tfrac{1}{4}A(G_1+G_3)\cos(\theta)\sin(\theta_{13})\\
&-\tfrac{1}{4}A(G_2+G_4)\sin(\theta)\sin(\theta_{24})\\
&-\tfrac{1}{4}A(G_1-G_3)\sin(\theta)\cos(\theta_{13})\\
&-\tfrac{1}{4}A(G_2-G_4)\cos(\theta)\cos(\theta_{24})
\end{aligned}
$$

where

$$
\begin{aligned}
\theta &\triangleq \tfrac{1}{4}(\theta_1-\theta_2+\theta_3-\theta_4)\\
\theta_{13} &\triangleq \tfrac{1}{2}(\theta_1-\theta_3) \qquad \theta_{24} \triangleq \tfrac{1}{2}(\theta_2-\theta_4).
\end{aligned}
$$

APPENDIX III

This appendix gives brief proofs of Facts 1, 2, 3 and 4.

Proof of Fact 1: It follows from (3) that the total output power P_{out1} is given by

$$
\begin{aligned}
P_{\text{out1}} &= \tfrac{1}{2}(A_s^2+A_n^2)+os_{cm}^2+os_{\text{diff}}^2\\
&= \tfrac{1}{2}A^2G^2(1+\alpha^2)+\tfrac{1}{4}[(os_1+os_2)^2+(os_1-os_2)^2]\\
&= \tfrac{1}{4}A^2(G_1^2+G_2^2)+\tfrac{1}{2}(os_1^2+os_2^2).
\end{aligned}
$$

Proof of Fact 2: It follows from (6) that the total output power P_{out2} is given by

$$
\begin{aligned}
P_{\text{out2}} &= \tfrac{1}{2}(A_{s4}^2+A_{n1}^2+A_{n2}^2+A_{n3}^2)\\
&\quad+\tfrac{1}{16}(os_1-os_2+os_3-os_4)^2\\
&\quad+\tfrac{1}{8}[(os_1-os_3)^2+(os_2-os_4)^2]\\
&\quad+\tfrac{1}{16}(os_1+os_2+os_3+os_4)^2\\
&= \tfrac{1}{8}A^2(G_1^2+G_2^2+G_3^2+G_4^2)\\
&\quad+\tfrac{1}{4}(os_1^2+os_2^2+os_3^2+os_4^2).
\end{aligned}
$$

Proof of Fact 3: It follows from (10) that the total output power P_{out3} is given by

$$
\begin{aligned}
P_{\text{out3}} &= \tfrac{1}{2}(B_s^2+B_n^2)\\
&= \tfrac{1}{8}(G_c^2+G_d^2)\\
&= \tfrac{1}{8}[(G_1-G_2)^2+(G_1+G_2)^2]\\
&= \tfrac{1}{4}(G_1^2+G_2^2)\\
&= \frac{1}{4}A^2\left[\frac{1}{1+(f_{\text{in}}/f_{c1})^2}+\frac{1}{1+(f_{\text{in}}/f_{c2})^2}\right].
\end{aligned}
$$

Proof of Fact 4: It follows from (12) that the total output power P_{out4} is given by

$$P_{\text{out4}} = \frac{1}{2}\left(B_{s4}^2 + B_{n1}^2 + B_{n2}^2 + B_{n3}^2\right)$$
$$= \frac{1}{8}A^2\left[\frac{1}{1+(f_{\text{in}}/f_{c1})^2} + \frac{1}{1+(f_{\text{in}}/f_{c2})^2}\right.$$
$$\left. + \frac{1}{1+(f_{\text{in}}/f_{c3})^2} + \frac{1}{1+(f_{\text{in}}/f_{c4})^2}\right].$$

ACKNOWLEDGMENT

REFERENCES

[1] C. Schiller and P. Byrne, "An 4 GHz 8b ADC system," *IEEE J. Solid-State Circuits*, vol. 26, pp. 1781–1789, Dec. 1991.

[2] M. McTigue and P. J. Byrne, "An 8-Gigasample-per-second 8-bit data acquisition system for a sampling digital oscilloscope," *Hewlett-Packard J.*, pp. 11–13, 1993.

[3] K. Poulton, K. L. Knudsen, J. Kerley, J. Kang, J. Tani, E. Cornish, and M. VanGrouw, "An 8-GSa/s 8-bit ADC system," in *Tech. Dig. VLSI Circuits Symp.*, Kyoto, June 1997, pp. 23–24.

[4] C. S. G. Conroy, D. W. Cline, and P. R. Gray, "An 8b 85MS/s parallel pipeline A/D converter in 1 μm CMOS," *IEEE J. Solid-State Circuits*, vol. 28, pp. 447–455, April 1993.

[5] K. C. Dyer, D. Fu, S. H. Lewis, and P. J. Hurst, "An analog background calibration technique for time-interleaved analog-to-digital converters," *IEEE J. Solid-State Circuits*, vol. 33, pp. 1912–1919, Dec. 1998.

[6] D. Fu, K. C. Dyer, S. H. Lewis, and P. J. Hurst, "A digital background calibration technique for time-interleaved analog-to-digital converters," *IEEE J. Solid-State Circuits*, vol. 33, pp. 1904–1911, Dec. 1998.

[7] W. C. Black Jr. and D. A. Hodges, "Time interleaved converter arrays," *IEEE J. Solid-State Circuits*, vol. 15, pp. 1022–1029, Dec. 1980.

[8] H. Kobayashi, M. Morimura, K. Kobayashi, and Y. Onaya, "Aperture jitter effects on wideband sampling systems," in *Proc. IEEE Instrumentation and Measurement Tech. Conf.*, Venice, May 1999, pp. 880–885.

[9] Y.-C. Jeng, "Digital spectra of nonuniformly sampled signals: Fundamentals and high-speed waveform digitizers," *IEEE Trans. Instrum. Meas.*, vol. 37, pp. 245–251, June 1988.

[10] A. Petraglia and S. K. Mitra, "Analysis of mismatch effects among A/D converters in a time-interleaved waveform digitizers," *IEEE Trans. Instrum. Meas.*, vol. 40, pp. 831–835, Oct. 1991.

[11] A. Montijo and K. Rush, "Accuracy in interleaved ADC system," *Hewlett-Packard J.*, pp. 38–46, 1993.

[12] N. Kurosawa, H. Kobayashi, and K. Kobayashi, "Channel linerity mismatch effects in time-interleaved ADC systems," in *Proc. Int. Symp. Circuits and Systems*, Sydney, Australia, to be published.

Haruo Kobayashi (S'88–M'89) received the B.S. and M.S. degrees in information physics from University of Tokyo, Japan, in 1980 and 1982, respectively, the M.S. degree in electrical engineering from University of California, Los Angeles, in 1989, and the Dr. Eng. degree in electrical engineering from Waseda University, Tokyo, Japan, in 1995.

He joined Yokogawa Electric Corporation, Tokyo, Japan in 1982, where he was engaged in the research and development related to measuring instruments and mini-supercomputers. In 1997, he joined Gunma University, Kiryu, Japan, and presently is an Associate Professor in the Electronic Engineering Department there. He was also an Adjunct Lecturer at Waseda University from 1994 to 1997. His research interests include analog and digital integrated circuit design and signal processing algorithms.

Dr. Kobayashi is a recipient of the 1994 Best Paper Award from the Japanese Neural Network Society.

Kaoru Maruyama received the B.S. and M.S. degrees in electronic engineering from Gunma University, Kiryu, Japan, in 1998 and 2000, respectively.

In 2000, he joined Matsushita Systems and Technology Company, Ltd. Kawasaki, Japan. His research interests include analog integrated circuit design and signal processing algorithms.

Hidetake Sugawara received the B.S. degree in electronic engineering from Gunma University Kiryu, Japan, in 1999, and is currently pursuing the M.S. degree in electronic engineering at the same University.

His research interests include ADC testing and analog integrated circuit design.

Naoki Kurosawa received the B.S. degree in electronic engineering from Gunma University, Kiryu, Japan, in 2000, and is currently pursuing the M.S. degree in electronic engineering in the same university.

His research interests include analog integrated circuit design.

Kensuke Kobayashi received the B.S. degree in electronic engineering from the University of Tokyo, Japan, in 1971.

In 1971 he joined the IWATSU Electric Company Ltd., Tokyo, Japan, where he was engaged in designing wideband sampling oscilloscopes. Since 1993, he has been developing fast-sampling-rate and wideband data acquisition systems in Teratec Corporation.